ELSEVIER

Biochimica et Biophysica Acta 1234 (1995) 139–143

BBA Biochimica et Biophysica Acta

Rapid Report

Energy-dispersive X-ray reflectivity study of the model membranes at the air/water interface

Ulrich Vierl [a], Gregor Cevc [a,*], Hartmut Metzger [b]

[a] *Medizinische Biophysik, Technische Universität München, Klinikum rechts der Isar, Ismaningerstr. 22, D-81675 Munich, Germany*
[b] *Sektion Physik, Ludwig Maximilians-Universität München, Geschwister Scholl Platz 1, D-80539 Munich, Germany*

Received 18 August 1994; accepted 8 December 1994

Abstract

The results of the first energy-dispersive reflectivity measurements with a (membrane coated) liquid surface are reported. They rely on the calibration curve measured with pure water and can be done without any sample or detector movement with a low-intensity, laboratory-based X-ray generator within less than 1 h. As an illustration, the structural parameters of a diarachidoylphosphatidylcholine monolayer at the air/water interface are determined. It is argued that the energy-dispersive detection in combination with the intense synchrotron radiation can be used for the time-resolved reflectivity measurements on the time-scale of minutes.

Keywords: Lipid monolayer; Membrane structure; Molecular packing; Phosphatidylcholine; Kinetic measurement

The technique of X-ray and neutron reflectivity is well established for the investigation of solid and liquid surfaces and surface layers (for an overview see Ref. [1]). During one measurement the reflectivity decreases at least 7 decades; therefore special care has to be taken to keep the background radiation small. For the air/water interface the first reflectometric measurements were therefore done with monochromatic X-rays from a synchrotron source [2]. Later on it was shown that the intensity of the X-radiation produced by a laboratory based generator, with rotating anode or sealed tubes, suffices for this purpose [3]. Good counting statistics then necessitates exposure times of many hours, however. This precludes kinetic measurements on the time scale of restructuring and of phase transitions in lipid layers on water, for example. A further disadvantage of the standard X-ray reflectometry experiments is that all angular positions must be controlled very accurately (sub mrad region) by keeping the sample surface horizontal. This makes experimental set-ups for the standard reflection measurements complex and costly.

To overcome these problems we have developed a versatile, laboratory-based diffractometer [4] suitable for reflectivity measurements with solid and liquid surfaces. It can be used both in the angle- (AD) and energy-dispersive (ED) mode. Here we demonstrate some of the advantages of ED reflectivity measurements, used for the first time for the investigation of surface layers on liquids.

Experimental details. Our X-ray reflectometer is based on an X-ray generator equipped with a 3 kW (Mo) sealed tube. A solid-state detector with a high purity Ge-crystal

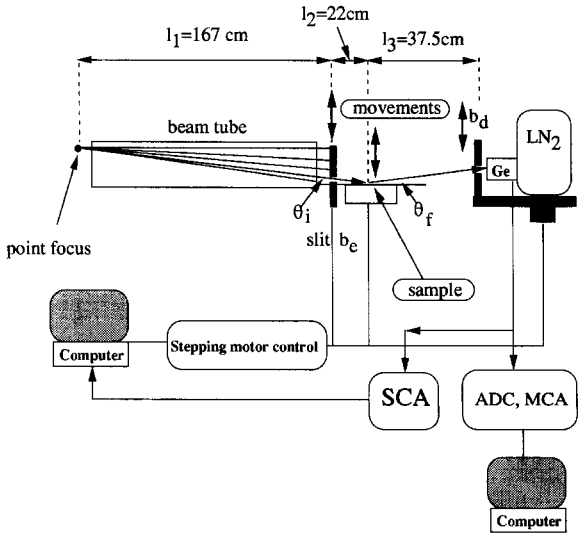

Fig. 1. Schematic side-view of the vertical reflectometer set-up, as used in our experiments.

* Corresponding author. Fax: +49 89 41404819.

SSDI 0005-2736(94)00320-3

and an excellent energy resolution of about 1% is used either as a 'monochromator' (for the AD measurements) or as an energy analyzer (for the ED experiments). The instrumental set-up used for this study is outlined in Fig. 1. The incident beam is selected from a widely distributed incoming radiation by moving the entrance slit S_e up or down. The position of the sample surface is selected so that the incident beam hits (and is reflected from) the sample center. The intensity of the reflected beam is recorded through a receiving slit S_r which is located so as to fulfill the condition of specular reflection. The distances between all individual instrument components are optimized with regard to the accuracy needed for a proper reflectivity measurement. More instrumental details are given elsewhere [4].

In order to measure surface reflectivity as a function of the vertical momentum transfer, $q_z \approx 4\pi(\sin\theta_i)/\lambda$, ($\theta_i$ being the angle of incidence and λ the wavelength), the reflectometer can be used in two modes. In AD measurements the vertical positions of slits and sample are changed stepwise so as to fulfill the specular condition; simultaneously, the scattered Mo-K_α-lines are selected from the spectrum by a single-channel analyzer, exploiting the high energy-resolution of the detector. In ED measurements the value of q_z is changed by the energy variation of the X-radiation, using the white spectrum of the tube. The reflected intensity is then determined by a multi-channel-analyzer as a function of the energy between the detection limit of our Ge-detector (5 keV) and the maximum of Bremsstrahlung (at about 40 keV). While in the AD measurement the reflectivity curve is recorded in a series of steps, in the ED measurement the whole reflectivity curve is obtained in one 'shot'. ED measurements are therefore unaffected by the variations in the intensity of the X-ray source, in contrast to AD measurements.

The problem with directly measured 'energy dispersive' reflectivity curves is that they are obscured by several perturbing, energy-dependent effects, such as the energy distribution of the tube spectrum, the detector sensitivity, etc. The directly measured data, therefore, have to be corrected for these effects, prior to final analysis. We routinely apply the following procedure for this purpose.

Calibration method. The intensity of the specularly reflected beam, as recorded in an ED measurement, is related to the surface reflectivity R by the following equation:

$$I(E) = R(q_z)\, g(E) \tag{1}$$

The function $g(E)$ is given by the product of the unknown energy distribution of the spectrum of the X-ray tube used, the detector sensitivity, and a function which allows for all secondary energy-dependent effects. (The latter largely stem from the diffuse X-ray scattering on water, the air, and the water vapour.) q_z is a function of the X-ray energy and the fixed angle θ_i. In order to get the required information about $g(E)$ one first measures the reflectivity $R(q_z)$ of a calibration sample in the AD mode. Next, the energy spectrum of the specularly reflected intensity, $I(E)$, is recorded at some suitably chosen specular angle. The calibration function $g(E)$ is found by means of Eq. (1) from these independently determined functions $I(E)$ and $R(q_z)$ after background subtraction. This simple procedure is only valid for a point-like resolution. In reality, however, both in the AD and ED measurements the recorded intensity is integrated over a finite volume of the resolution elements $V_{ad}(q)$ and $V_{ed}(q)$, respectively. The influence of different resolution elements on the collected intensity is thus important for the choice of an appropriate reflection angle in the ED mode and deserves some more discussion.

From simple geometric considerations the following expressions for the three-dimensional volume element of resolution in the reciprocal space are found:

$$\Delta q_x \cdot \Delta q_y = \frac{q}{2}(\Delta\theta_i + \Delta\theta_f) \cdot \frac{q}{2\sin\theta_i}(\Delta\phi_i + \Delta\phi_f) \tag{2}$$

$$\Delta q_z = \frac{q}{2}(\Delta\theta_i + \Delta\theta_f) \cdot \cot\theta_i + q \cdot \frac{\Delta\lambda}{\lambda} \tag{3}$$

$\Delta\theta_i$ and $\Delta\theta_f$ are the vertical divergences of the incident (i) and final (f) beams, respectively, while $\Delta\phi_i$ and $\Delta\phi_f$ are the corresponding horizontal divergences. They can be calculated from the slit widths and distances as given in Fig. 1.

Meaningful reflectivity measurements necessitate the use of proper background correction. Such correction is done by setting the detector in two off-specular positions close to $\theta_i = \theta_f$ at each q_z. From this, the background at the specular position is interpolated and subtracted from the specular measured intensity. This correction already includes a compensation for the variability of q in the x- and y-direction. This leaves Δq_z (Eq. (3)) as the only relevant dimension of the resolution element. In any AD measurement $\Delta\lambda/\lambda$ is a constant. Its value is given approximately by the separation of the $K_{\alpha 1}$ and $K_{\alpha 2}$ lines ($\Delta\lambda/\lambda = 6.01 \cdot 10^{-3}$). The resolution of our Ge-detector at this energy is about twice this value. For the ED measurements $\Delta\lambda/\lambda$ thus decreases with increasing energy, E, like $\Delta\lambda/\lambda \approx 2.3 \cdot E^{-1/2}$.

Summing up all the known contributions to the resolution element in the reciprocal space, it can easily be shown that AD-resolution equals to that of an ED-measurement done at $q_z \simeq 9q_c$ (q_c is the critical q_z-value for the total reflection of X-rays on water). This angle is thus conveniently chosen for the ED measurements. It is a good compromise between the desire to use large scattering angles (corresponding to a large region of $q \sim \sin\theta$) and the need to decrease the diffuse background scattering by working at small reflection angles. Our present instrumental set-up allows ED reflectometry measurements only for $q_z \leq 15q_c$. This limitation is chiefly due to the elastic and inelastic diffuse background scattering on water, water

vapour and on the surface capillary waves. While the signal from this background scattering increases approximately as q_z square [1], the specular intensity decreases approximately as q_z^4. The counting statistics at energies above about 20 keV, moreover, is very poor due to the low primary X-ray intensity.

Calibration- and test-measurements. Owing to its defined properties, the water/air interface provides an ideal system for the determination of the calibration function $g(E)$. Surface capillary waves provide no obstacle to this if they are suppressed by using very thin (< 300 μm) water films.

A typical water reflectivity curve, as measured in the AD mode, is shown in Fig. 3 (top right, open circles). It has been normalized with regard to the Fresnel reflectivity of an ideally smooth water surface, R_F, to emphasize the surface roughness effect. This curve looks as expected except in the low-angle region where the reflectivity values deviate from the simulated solid curve. This could be due to the X-ray scattering by the water vapour above the air/water interface. (Indeed, this effect is expected to be stronger at small angles, where the beam-path through the vapour-rich region is much longer than at high angles.) This conclusion is supported by the observation that the measured reflectivity at small angles decreases with increasing temperature, when the thickness and the density of the water vapour layer above the water surface also grow. Corrections for the background scattering are made for the low reflectivity values (i.e., for the scattering-vectors larger than $7q_c$) as described before.

The decrease of the normalized reflectivity curve, R/R_F, at high wave-vectors is due to the surface roughness. This is primarily due to the residual thermally excited capillary waves on the water surface. To describe this phenomenon one can smear-out the surface density profile by an error function. This is tantamount to introducing a Debye-Waller-like exponent into the expression for the calculation of the surface reflectivity outside the region of total reflection (see [1,6]):

$$R(q) = R_F(q) \cdot e^{-q^2\sigma^2} = \left(\frac{q^2 - \sqrt{q^2 - q_c^2}}{q^2 + \sqrt{q^2 - q_c^2}} \right)^2 \cdot e^{-q^2\sigma^2} \quad (4)$$

By fitting this expression (solid line) to the data of figure monolayer one gets $\sigma = (0.29 \pm 0.02)$ nm for the value of surface roughness parameter [2].

[1] The short-range order of water-molecules gives rise to a very broad peak at $q = 0.95(2\pi/a) \approx 88 q_c$, where $a \approx 0.31$ nm is the mean distance between two water molecules [5].

[2] The measured surface roughness parameter depends also on the resolution of the reflectivity apparatus and increases with decreasing resolution [2]. The theoretical limit is 0.15 nm.

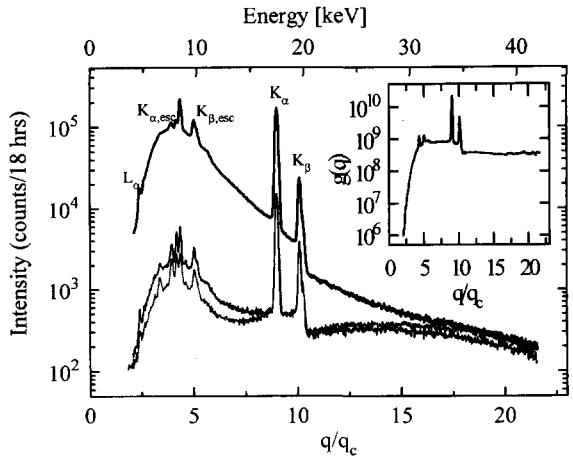

Fig. 2. Reflected X-ray intensity from an air/water interface as a function of energy (upper axis) or scattering vector, q/q_c (lower axis). The main reflectivity curve was measured at $\theta_i = 9\theta_c$ (thick curve) and the corresponding background scattering curves at $\theta_f = 9\theta_c - 0.2°$ ($\cdots$) and $\theta_f = 9\theta_c + 0.2°$ (—). The latter two curves are shown as thin lines. Inset: Calibration curve, $g(E)$ (see the text for details).

The reflectivity of the same water surface has also been measured in the ED mode at angle $9\theta_c$ ($\theta_c = 1.23$ mrad for Mo(K_α)). A typical result of this measurement is shown in Fig. 2. The nonspecular background scattering, determined at $\theta_f = \theta_{spec} \pm 0.20°$, is comparably strong as the specular intensity at q_z-values larger than 17.5. The proposed background subtraction then ceases to be meaningful. (The decreased intensity toward the low q-end is due to the vanishing detector efficiency near and below 3 keV.)

The characteristic molybdenum K-lines are observed in all spectra together with their corresponding escape peaks. The measured ED intensity data, as shown in Fig. 2, are first corrected for the background scattering and then converted onto q-scale. The resulting values are next divided by the corresponding reflectivity values, derived from the AD measurement according to Eq. (4), including the surface roughness parameter σ. The resulting calibration curve $g(E)$ is given in the inset to Fig. 2.

In order to test the quality of our measuring procedure we have determined the reflectivity of a DAPC monolayer at the air/water interface. DAPC has been spread from a chloroform solution at room temperature. The spread liquid quantity was chosen so as to give a dense monolayer with the packing parameters corresponding to those of a DAPC bilayer. The resulting background-corrected and -calibrated ('ED') reflectivity curve is presented in Fig. 3 (left bottom). The uncorrected (not shown) and corrected data are nearly identical at $q < 12\theta_c$. This suggests that no corrections are necessary in this scattering vector region. For $q \geq 15\theta_c$, however, the specular reflectivity is 'drowned' in the diffuse scattering signal. This region, therefore, is less useful for data analysis. This notwithstanding, the meaningful part of the measured reflectivity curve extends over a respectable range of q_z-values. It clearly reveals the minimum resulting from the interfer-

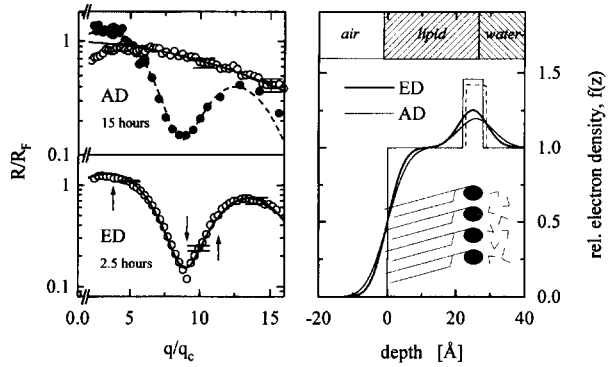

Fig. 3. Normalized reflectivity of the water/air and lipid/air interface at 25°C (symbols) together with the corresponding data fits (solid curves); errors are given as horizontal bars. Top left: water (○) and diarachidoylphosphatidylcholine monolayer (DAPC, ●), as measured by the AD method over 15 h. Bottom left: DAPC monolayer (○) as measured by the ED method (○) within 2.5 h. In the ED experiment, every point gives the mean of 12 channels. All reflectivities are normalized with regard to the Fresnel-reflectivity of an ideally smooth water surface and are corrected for the background scattering. Arrows show the positions of the characteristic Mo-lines. Right panel shows the results of the corresponding data analyses based on the Gaussian-smeared, two-box model for the electron density profile, $f(z)$.

ences that are brought about by the existence of a DAPC monolayer at the air/water interface. The insignificant 'contaminations' around $q/q_c = 4$, 9 and 10.8 are the remnants of the characteristic K-lines of molybdenum. These residuals are thus excluded from the data analysis for a proper fit. These 'contaminations' can be prevented by using a tungsten X-ray tube for ED measurements ($E_{K\alpha} = 58.87$ keV).

Surface reflectivity curves can be used to calculate the corresponding electron density profiles within the framework of a Gaussian smeared two-box model. The result of such a calculation for the DAPC monolayer is shown in Fig. 3 (right bottom). It proves that the calculated electron density profile of this lipid is very similar to the profiles obtained from the small-angle X-ray scattering measurements with DAPC multilayers in excess water. The thickness of the hydrocarbon region in a DAPC monolayer is $d_c = 2.14$ nm; the headgroup layer thickness is $d_h = 0.57$ nm. The results of the data fit are not unequivocal, however. A broad, Gaussian-smeared electron density box can not be distinguished from the sharp box with a higher, but more smeared-out electron density. Furthermore, the interface between the chain- and the headgroup regions is not well defined. It is therefore more reasonable to look at the nominal bilayer thickness than at the individual regions in a monolayer. In our case, the bilayer thickness adds up to $d_b = 2(d_c + d_h) = 2.71$ nm. This compares well with the result of X-ray small-angle diffractometry, which yields for the same lipid: $d_b = 2.60$ nm [7]. The small difference between these two values may be due to the different hydrocarbon tilt angles in both systems (see further discussion). (Neither of these two values contains the contribution from the hydrated choline group, which has a similar electron density as pure water.)

The counting statistics of data accumulated during a 2.5-h experiment shows that the ED detection yields results that have same or higher quality than those of a 15-h AD measurement (see Fig. 3). Data of similar quality as in the displayed AD measurement can be recorded within 0.5 h with ED detection (not shown). On the one hand, this is due to the simultaneous data-collection. On the other hand, one also gains from the averaging over many channels in the multi-channel-analyzer. The curve shown in Fig. 3, for example, was obtained by averaging the original data over 12 adjacent channels. Such a sampling interval is still smaller than the corresponding resolution element (number of all data points is 1024) and thus perfectly justified.

The electron density profiles obtained by these two methods are identical, within the limits of measurement precision [8]. The average box width of the chain region (22 ± 1.5 Å) suggests a value of $\sim(25 \pm 7)°$ for the tilt-angle of the chains in the all-*trans* conformation. For DAPC bilayers, a chain tilt of 35° was reported [9]. This somewhat higher value may be due to the small difference in the lipid conformation at the air/water interface or in the bulk, which is caused by the fact that tilt angle normally increases with the phospholipid hydration. It must be noted, that the measured smearing parameter depends on the resolution function of the apparatus and on the measuring method [2]. The observed 10%-variation of this parameter is therefore perhaps a systematic effect, although it is still in the range of the measurement precision.

Data shown in Fig. 3 were not corrected for the X-ray absorption effects. This is permissible in light of the low absorption edges (below ~ 3 keV) of lipid and most other biological materials (see also [10]). Absorption would result in fluorescence and thus in an increase of the background scattering, however. This would make background subtraction in AD as well as ED measuring mode problematic. Non-biological materials with absorption edges between 4 and 35 keV should, therefore, be investigated by the AD method and monochromatic X-rays far from the absorption edge. Alternatively, the technique of X-ray standing waves [11] should be used, where the X-ray excited fluorescence is even needed.

In summary, we have shown that the energy-dispersive measurements of the water surface reflectivity are possible at least for the wave-vector values $\leq 17.5 q_c$. Such measurements can be done rapidly, on the time scale of 0.5 to 1 h, even with an ordinary X-ray tube; this is an improvement by more than a factor of 5 over the angle dispersive measurements. In combination with the high intensity synchrotron-radiation sources (where the calibration should be much easier because of the purely white spectrum) even kinetic measurements on the time scale of minutes should be possible. Moreover, with some effort, the currently

accessible range of explorable wave-vectors could be expanded. This may open new frontiers in the research of liquid surfaces.

References

[1] Russell, T.P. (1990) Mater. Sci. Rep. 5, 171–271.
[2] Braslau, A., Pershan, P.S., Weiss, A.H., Als-Nielsen, J. and Bohr, J. (1985) Phys. Rev. Lett. 54, 114–117.
[3] Dalliant, J., Benattar, J.J. and Leger, L. (1990) Phys. Rev. A 41, 1963–1977.
[4] Metzger, T.H., Luidl, C., Pietsch, U. and Vierl, U., in press.
[5] Guinier, A. (1963) X-Ray Diffraction, W.H. Freeman, San Francisco.
[6] Helm, C.A., Tippmann-Krayer, P., Möhwald, H., Als-Nielsen, J. and Kjær, K. (1991) Biophys. J. 60, 1457–1476.
[7] Kirchner, S. and Cevc, G. (1995) submitted.
[8] Lösche, M. (1994) Habilitationsschrift, Johannes-Gutenberg-Universität, Mainz
[9] Tristram-Nagle, S., Zhang, R., Suter, R.M., Worthington, C.R., Sun, W.J. and Nagle, J.F. (1993) Biophys. J. 64, 1097–1109.
[10] Als-Nielsen, J. and Kjær, K. (1989) in The proceedings of the Nato Advances Study Institute, Phase Transitions in Soft Condensed Matter, Geilo, Norway, April 4–April 14, 1989 (Riste, T. and Sherrington, D., eds.), Plenum Press, New York.
[11] Bedzyk, M.J., Bilderback, D.H., Bommarito, G.M., Caffrey, M. and Schildkraut, J.S. (1988) Science 241, 1788–1791.